

# Background Reading Report

**Group 7:** Co-Robotic Ultrasound Imaging of Breast Assisting Mammography

**Students:** Julian Brown, Kevin Wang, Yuxin (Ethan) Chen

**Mentors:** Dr. Emad Boctor, Dr. Web Stayman, Dr. Russell Taylor, Yixuan Wu

## Background Reading Paper: Phantom with Multiple Active Points for Ultrasound Calibration

**Authors:** Haichong K. Zhang, Alexis Cheng, Younsu Kim, Qianli Ma, Gregory S. Chirikjian, Emad M. Boctor

### Reason for Paper Selection

This project focuses on building a robotic system for augmenting current mammography procedures with autonomous ultrasound imaging. In order to do this, a UR5 robotic arm has been fitted with a 3D-printed end-effector housing a camera as well as an ultrasound probe. Calibration of the camera with respect to the robot has been performed and validated, resulting in an accurate transformation between the end of the arm and the camera frame. A similar calibration must be performed to calibrate the ultrasound probe with the robotic arm. This paper details a technique for ultrasound probe calibration using multiple “active” points, which is more accurate than the traditional passive point or cross-wire calibration. This paper was selected to help determine which calibration method to use and how to do it successfully.

### Introduction

Ultrasound calibration is necessary when using ultrasound imaging in conjunction with robotics as it allows for the position of points of interest in the ultrasound images to be measured with respect to the robot end-effector and base frame. It also enables the ultrasound images to be stitched together accurately to create a more detailed and useful image.

Two different types of phantom have traditionally been used for ultrasound calibration: Point-based and Structural. Point-based calibration involves the use of a single point or multiple points of known locations within a 3D space. Structural phantoms, instead, have a continuous, predetermined structure on which the calibration is performed. Point-based phantoms are typically more accurate, although they can take longer to complete, and it can be more difficult to automate. Structural methods are generally less accurate, but easier to automate.

This paper proposes a third type of phantom called a Multiple Active Point (MAP) phantom. Instead of using passive points which simply reflect ultrasound waves back to the probe, a piezoelectric element can be used to transmit signals actively, reducing error due to background noise and reverberation, as well as allowing the probe to receive out-of-place signals.

### Theory

In calibration, the end goal is to compute transformation matrix  $X$ . This is the rigid-body transformation bridging the tracker frame and US image frame.  $X$  can be computed via two

methods,  $BXp = XB$  or  $AX = XB$  where  $A, X, B \in SE(3)$ , and  $p \in \mathbb{R}^3$  where  $B$  is is sensor reading,  $p$  is the location of a point in US coordinates, and  $A$  is the image pose

Again, there are benefits to both methods that I would like to discuss. If one is using a point based phantom with a single point, the  $BXp = XB$  method is used. This is because a single point provides positional information, but does not provide the full pose – that is, rotational information is not present. You can visualize this with the figure below, in (Fig 1. a), no matter what pose the US probe is put into, the rotational information of the point is constant as it is a uniform point in space. On the other hand, with a structure in (b), acquiring data from different US probe poses results in different rotational configurations of your object, allowing for the closed form and faster  $AX=XB$  computation. Again, this speed tradeoff comes at the price of accuracy, the  $BXp$  formulation provides a more accurate calibration.

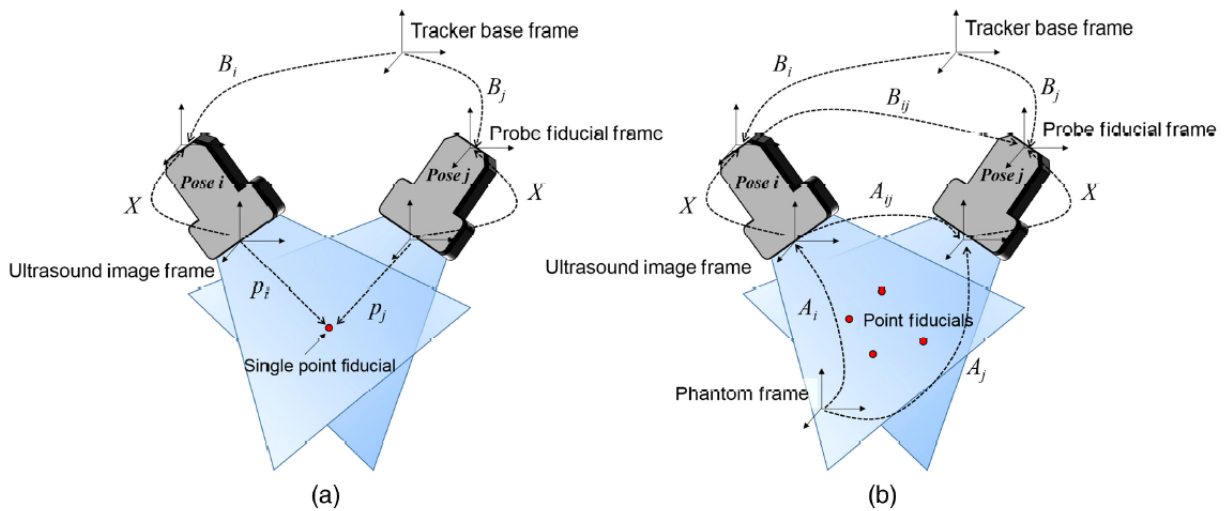


**Fig. 1** Illustration of coordinate systems on ultrasound calibration. (a) A single point target phantom, in which  $BXp$  formulation is used. (b) The proposed MAP phantom, in which  $AX = XB$  formulation is used.

Zhang's proposed Multiple Active Point Phantom, uses a concept developed by Cheng and Guo et al, the Active Point, where a point emits the acoustic wave for the US probe to capture, as opposed to the classic passive point. This provides background free signals and reduces noise, and in turn allows for more precise midplane searching. However, the search is still time consuming. This is where Zhang's extension takes effect; by using multiple active points, different US probe poses produce different image poses. Now we have the translational and rotational information required to use the faster  $AX=XB$  formulation, while still taking advantage of the accurate point based phantom.

## Materials and Methods

Materials:

- UR5 robotic arm
- BPL9-5/55 Transrectal Bi-plane Ultrasonix Probe
- SonixDAQ data-recording device
- 1-mm disc-shaped piezoelectric element

## Methods

As shown in Figure ##, 12 MAP phantom designs were tested in this experiment. The number and spacing of the points were varied to determine the optimal setup. 125 robotic poses were used for each design. Of those, 60 were randomly chosen for the calibration, and 60 of the remaining poses were used for evaluation. It is important to note that only one real active element was used. The other points were actually simulated by moving the robot translationally within each pose.

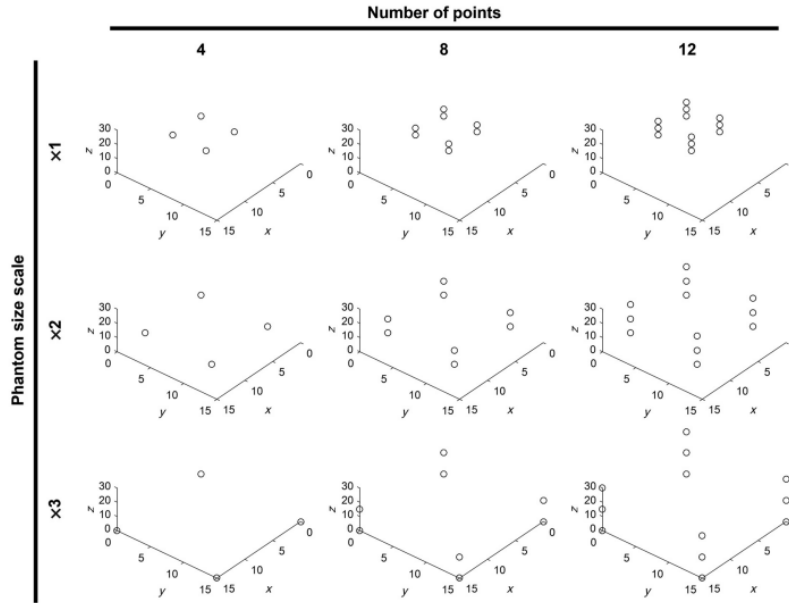


Figure 2- Simulated phantom designs. The size scale (1, 2, 3 times), starting at 5 mm, and number of points (4, 8, 12) were varied.

Both accuracy and precision were used to evaluate each calibration. The equations are shown below:

$$\sigma_{Accu} = \left| \frac{1}{N} \sum_{i=1}^N (B_i X p_i - c) \right|_2$$

$$\sigma_{RP} = \left| \sqrt{\frac{1}{N} \sum_{i=1}^N (B_i X p_i - \overline{B X p})^2} \right|_2$$

In the accuracy equation,  $c$  is the ground-truth target point. In the precision equation, the  $\overline{B X p}$  term is the mean of all  $B_i X p_i$ . In this way, the accuracy metric is essentially finding the average difference between each point's location calculated through the calibration result and its true location, and the precision metric is finding the average difference between each point's location calculated through the calibration result and the average location of each calibration estimate.

## Results

Accuracy and precision for each phantom design were evaluated with segmentation error and out-of-plane error added separately. Segmentation error is error in the image plane axes. Out-of-plane error is error in the elevation axis (see Figure 3)

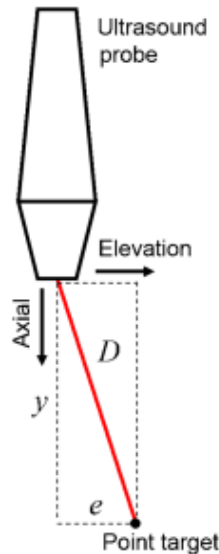


Figure 3- Ultrasound image coordinate axes with the image plane running perpendicular to the page.

The results for each design are shown in the table below.

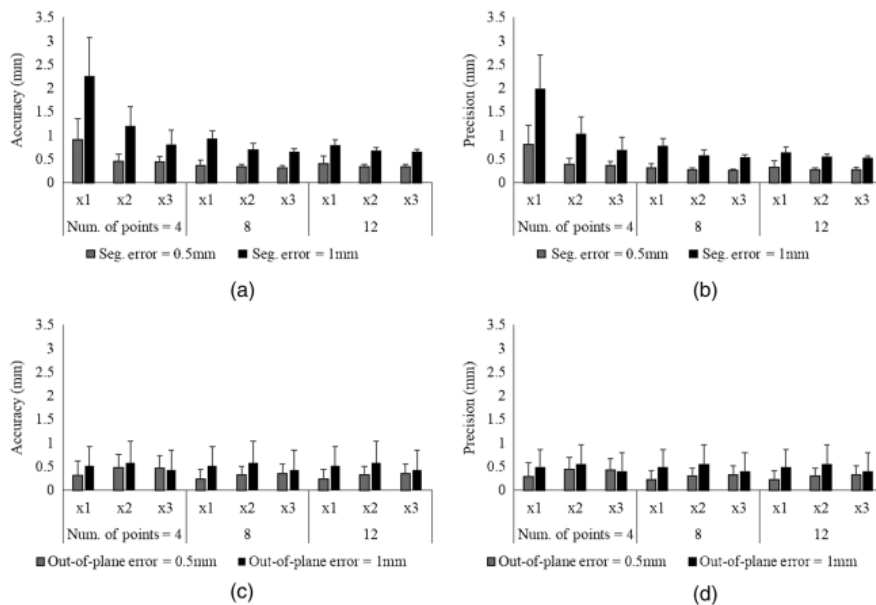


Figure 4- Accuracy and precision metric results for each MAP phantom design with segmentation and out-of-plane error added separately.

With segmentation error, accuracy and precision both improved with increased spacing and number of points, as expected, although differences between 8 and 12 points were minimal. With out-of-plane error, accuracy and precision stayed consistent regardless of the spacing and number of points.

### Comparison with Cross Wire Phantom

The calibration performance of MAP phantom and cross wire phantom was compared in this paper. Cross wire phantom has its advantage on easy to set up, cheap and also provide a good calibration performance. The radius of flushing line in cross wire phantom is 0.1mm, which is smaller than the ultrasound resolution. Thus, the cross point can be set as an ideal point in the ultrasound image, which leads to high accuracy calibration performance.

The calibration performance of cross wire was listed in the table below at the second last line. As shown in the table, MAP phantom provide a higher precision on calibration performance.

Calibration		Internal precision <i>c</i> (mm)	External precision <i>c</i> (mm)
Dual array (biplane)	<i>BXp</i> Point #1	0.77	2.55
	<i>BXp</i> Point #2	0.68	1.56
	<i>BXp</i> Point #3	0.79	3.59
	<i>BXp</i> Point #4	0.66	2.60
	<i>AXXB</i>	0.60	0.67
Mono (1-D) array	<i>AXXB</i>	0.93	0.98
Control ( <i>BXp</i> ) <sup>14</sup>	<i>CW/AE</i>	1.72	—
	<i>AE/CW</i>	1.00	—

Figure 5- Experiment results for calibration performance by using MAP phantom and other phantom.

### Assessment:

#### (1) About This paper

##### Pros:

For the MAP phantom proposed in the paper, the strength of this phantom is that it can improve calibration performance to achieve higher accuracy and precision than cross-wire phantom and AE phantom. Meanwhile, MAP phantom can also reduce the number of midplane detection processes necessary thus decreasing the data acquisition time during US calibration.

##### Cons:

The weakness of of the MAP phantom is that the fabrication of a MAP phantom requires a special hardware setup including multiple active US elements. In specific, Multiple Active US elements with known geometric relationships are required. Or, one Active US element and an extra translational step for each pose to simulate the presence of extra points (this also adds error) are necessary to fabricate a MAP phantom. Another con of this proposed concept is that it was derived in theory and was demonstrated through simulation and experiment. In the future,

the proposed MAP phantom can be simplified and integrated into a compact package that is readily available for calibration.

## **(2) About Our Project**

The main takeaways from this paper is that MAP phantom provide us a method to achieve high US calibration performance. Evaluation method used in this paper can be used to evaluate our US calibration performance. Our project does not require high accuracy US calibration as we are using cameras to direct the movement of our robot. MAP phantom calibration is probably outside of our scope, but we will keep in mind, if it turns out higher accuracy calibration is needed for whatever reason.

## **Reference**

Zhang HK, Cheng A, Kim Y, Ma Q, Chirikjian GS, Boctor EM. Phantom with multiple active points for ultrasound calibration. *J Med Imaging (Bellingham)*. 2018 Oct;5(4):045001. doi: 10.1117/1.JMI.5.4.045001. Epub 2018 Nov 27. PMID: 30525061; PMCID: PMC6257090.